# Preparation and Crystal Structures of Ternary Rare Earth Silver and Gold Arsenides $LnAgAs_2$ and $LnAuAs_2$ with $Ln$ = La–Nd, Sm, Gd, and Tb

Marcus Eschen and Wolfgang Jeitschko

Institut für Anorganische und Analytische Chemie, Westfälische Wilhelms-Universität Münster, Wilhelm-Klemm-Straße 8, D-48149 Münster, Germany

Reprint requests to W. Jeitschko. Fax +49-(0)251-83-33136. E-mail: jeitsch@uni-muenster.de

Z. Naturforsch. **58b,** 399 – 409 (2003); received November 28, 2002

*Dedicated to Professor Mewis on the occasion of his 60th birthday*

The 14 arsenides $LnAgAs_2$ and $LnAuAs_2$ ($Ln$ = La–Nd, Sm, Gd, Tb) were prepared by reaction of stoichiometric mixtures of the elemental components at high temperatures and characterized by X-ray diffractometry. The silver compounds $LaAgAs_2$ and $CeAgAs_2$ and the gold compounds $LnAuAs_2$ ($Ln$ = Ce–Nd, Sm, Gd, Tb) crystallize with $HfCuSi_2$ type structure ($P4/nmm$, $Z$ = 2). Of these, the structures of $CeAgAs_2$ ($a$ = 408.5(1), $c$ = 1048.2(1) pm, conventional residual $R$ = 0.017 for 261 structure factors and 12 variable parameters) and $CeAuAs_2$ ($a$ = 411.4(1), $c$ = 1015.3(2) pm, $R$ = 0.030 for 428 $F$ values) were refined from four-circle diffractometer data. The silver compounds $LnAgAs_2$ ($Ln$ = Pr, Nd, Sm, Gd, Tb) are isotypic with the antimonide $SrZnSb_2$ ($Pnma$, $Z$ = 4) as demonstrated by a single-crystal structure refinement of $PrAgAs_2$ ($a$ = 2107.3(4), $b$ = 401.7(1), $c$ = 407.8(1) pm, $R$ = 0.042 for 746 $F$ values and 26 variables). The gold compound $LaAuAs_2$ ($I4/mmm$, $Z$ = 4, $a$ = 416.9(1), $c$ = 2059.5(3) pm, $R$ = 0.038 for 303 $F$ values and 13 variables) was found to be isotypic with the bismuthide $SrZnBi_2$, again by a refinement from single-crystal diffractometer data. In the structures of $CeAgAs_2$, $LaAuAs_2$, and $CeAuAs_2$ large displacement parameters perpendicular to the four-fold axes were found for one of the two arsenic positions. These structures could also be refined with split positions for these arsenic atoms, which allow for considerable As–As bonding, resulting in a formal charge of $-1$ for these atoms. Chemical bonding in these compounds can thus be rationalized by a simple model corresponding to the formula $Ln^{+3}T^{+1}As^{-1}As^{-3}$ ($T$ = Ag, Au), where the superscripts indicate oxidation numbers.

*Key words:* Rare Earth Compounds, Arsenides, Crystal Structure

## Introduction

The ternary silicide $HfCuSi_2$ [1] and the quarternary silicide arsenide ZrCuSiAs [2], both crystallize with the tetragonal space group $P4/nmm$ and four corresponding atomic positions. Villars and Calvert [3] consider these structures to be isotypic (ZrCuSiAs type) while Parthé and coworkers [4] distinguish between the structures of the ternary and the quaternary compounds. Similarly, the binary aluminide $BaAl_4$ [5] and the ternary silicide $ThCr_2Si_2$ [6] (including the "anti"-type structure reported for the telluride oxide $Nd_2TeO_2$ [7] and the antimonide nitride $U_2SbN_2$ [8]) crystallize with three corresponding atomic positions in the tetragonal space group $I4/mmm$. Again, Parthé and coworkers consider the binary and ternary compounds to crystallize with two different structure types, while for Villars and Calvert $ThCr_2Si_2$ has a $BaAl_4$ type structure. Incidentally, there is agreement that the truly body centered structure of elemental tungsten and the (frequently, but erroneously called body centered) CsCl type structure represent two different structure types, since their space group symmetries ($Im\bar{3}m$ and $Pm\bar{3}m$, respectively) are different.

Irregardless of whether only ternary compounds with $ThCr_2Si_2$ type structure are counted, or whether the binary $BaAl_4$ type compounds are included, this simple tetragonal structure type is the one with the largest number of representatives: almost 800 [3, 9 – 13]. Similarly, the structures of ZrCuSiAs and $HfCuSi_2$ may even reach a higher count because of their equal simplicity and because they offer four different atomic positions, all of which may be occupied by a large number of different elements. Almost 300

compounds with ZrCuSiAs (or HfCuSi$_2$) type structure are known already [14,15 and references therin]. Most recent additions are the quaternary rare earth and bismuth copper chalcogenide oxides *A*Cu*Ch*O (*A* = *Ln*, Bi; *Ch* = S, Se, Te) [16], PrCuSO [17], the rare earth zinc pnictide oxides *Ln*Zn*Pn*O (*Pn* = P, As) [18], the corresponding cadmium compounds *Ln*Cd*Pn*O [19], the chalcogenide fluorides EuCuSF [20] and SmCuSeF [21], and the silicide phosphide ZrCuSiP [22].

Here we report on ternary rare earth silver and gold arsenides with HfCuSi$_2$ type and related structures. Several ternary pnictides containing the coinage metals copper, silver, and gold with the composition 1:1:2 or close to that have already been characterized in recent years. Mewis was the first reporting EuCu$_{2-x}$P$_2$ to crystallize with a defect-ThCr$_2$Si$_2$ type structure [23]. An independent structure refinement of this phase resulted in a very low copper content corresponding to the formula EuCu$_{1.622(6)}$P$_2$ [24]. For the other rare earth copper phosphides with the general formula *Ln*Cu$_{1\pm x}$P$_{2\pm y}$ (*Ln* = La – Nd, Sm, Gd – Tm) [24 – 31] several structures have been reported which are isotypic with or closely related to those of HfCuSi$_2$ [1], SrZnSb$_2$ [32], SrZnBi$_2$ [33], U$_3$Ni$_{3.34}$P$_6$ ("UNi$_{1.11}$P$_2$") [34], Pr$_3$Zn$_2$As$_6$ ("PrZn$_{0.67}$As$_2$") [35], and CeAg$_{1.08}$P$_{1.87}$ [36]. Similar structures have also been determined from single-crystal data of various compositions of the solid solution series SmCu$_{1+\delta}$As$_{2-x}$P$_x$ [37], GdCuAs$_{2-x}$P$_x$ [38], HoCuAs$_{2-x}$P$_x$ [39], and ErCuAs$_{2-x}$P$_x$ ($x$ = 0 – 2) [39]. This is also the case for the series of the ternary rare earth copper arsenides *Ln*Cu$_{1+x}$As$_2$ ($x$ = 0.00 – 0.25) where the structures may depend on the copper contents [14, 37 – 42]. The corresponding antimonides *Ln*CuSb$_2$ are reported to crystallize with HfCuSi$_2$ type structure [43 – 47], and this structure has also been established for the bismuthide CeCu$_{0.706(1)}$Bi$_2$ [48].

As compared to the ternary rare earth copper pnictides, the corresponding silver and gold compounds have not yet received that much attention. X-ray powder data indicate HfCuSi$_2$ type related structures for the three phosphides *Ln*AgP$_{2+x}$ (*Ln* = La – Pr) [24, 26, 27]. For the rare earth silver antimonides *R*AgSb$_2$ (*R* = Y, La – Nd, Sm, Gd – Tm) the HfCuSi$_2$ type structure has been reported [14, 44, 49 – 52]. This structure has also been found for the five rare earth gold antimonides *Ln*AuSb$_2$ (*Ln* = La – Nd, Sm) [43, 53]. Here we publish the results of our investigations about corresponding ternary silver and gold arsenides. The gold arsenides *Ln*AuAs$_2$ are new compounds. In contrast, the silver compounds *Ln*AgAs$_2$ have already been prepared by Möller [24], but details about their characterization from X-ray powder data have not been published in the open literature. Demchyna, Kuz'ma, and Babizhetsky have prepared these compounds independently [54]. From X-ray powder data they found LaAgAs$_2$ and CeAgAs$_2$ to crystallize with the tetragonal HfCuSi$_2$ type structure, which we confirm by a single-crystal investigation of CeAgAs$_2$. For the other arsenides *Ln*AgAs$_2$ (*Ln* = Pr, Nd, Sm, Gd – Dy) these authors reported an orthorhombic distortion of that structure. Our single-crystal structure determination of PrAgAs$_2$ resulted in the closely related orthorhombic SrZnSb$_2$ type structure in agreement with Möller's findings [24].

Table 1. Lattice constants of ternary arsenides *Ln*AgAs$_2$ and *Ln*AuAs$_2$ with HfCuSi$_2$ ($P4/nmm$), SrZnSb$_2$ (*Pnma*), and SrZnBi$_2$ ($I4/mmm$) type structure, respectively.

| Compound | Space group | *a* [pm] | *b* [pm] | *c* [pm] | *V* [nm$^3$] |
|---|---|---|---|---|---|
| LaAgAs$_2$ | $P4/nmm$ | 411.07(5) | | 1063.0(1) | 0.17963(5) |
| CeAgAs$_2$ | $P4/nmm$ | 408.45(3) | | 1048.2(1) | 0.17487(4) |
| PrAgAs$_2$ | *Pnma* | 2107.3(4) | 401.66(6) | 407.81(7) | 0.3452(2) |
| NdAgAs$_2$ | *Pnma* | 2099.3(3) | 400.43(9) | 404.69(9) | 0.3402(2) |
| SmAgAs$_2$ | *Pnma* | 2096.3(3) | 398.01(8) | 401.83(7) | 0.3353(2) |
| GdAgAs$_2$ | *Pnma* | 2091.9(5) | 395.84(9) | 398.87(8) | 0.3303(2) |
| TbAgAs$_2$ | *Pnma* | 2088.8(4) | 393.63(9) | 394.48(8) | 0.3244(2) |
| LaAuAs$_2$ | $I4/mmm$ | 416.90(5) | | 2059.5(3) | 0.3579(1) |
| CeAuAs$_2$ | $P4/nmm$ | 411.35(5) | | 1015.3(2) | 0.17180(8) |
| PrAuAs$_2$ | $P4/nmm$ | 408.97(6) | | 1021.2(1) | 0.17080(8) |
| NdAuAs$_2$ | $P4/nmm$ | 407.9(1) | | 1019.0(4) | 0.1695(2) |
| SmAuAs$_2$ | $P4/nmm$ | 403.94(5) | | 1016.9(2) | 0.16593(7) |
| GdAuAs$_2$ | $P4/nmm$ | 401.60(5) | | 1014.8(3) | 0.16367(9) |
| TbAuAs$_2$ | $P4/nmm$ | 399.85(5) | | 1009.9(1) | 0.16146(6) |

## Sample Preparation and Lattice Constants

The samples were prepared by reaction of the elemental components in the atomic ratio 1:1:2. Starting materials were ingots of the rare earth elements, silver and gold in the form of wires, and arsenic granules, all with nominal purities of at least 99.9%. The arsenic was further purified by fractional sublimation prior to the reactions. Cold-pressed pellets of the elements were sealed into evacuated silica tubes. These tubes were heated to 400 °C, held at that temperature for 16 h and further heated at a rate of 5 °C/h to 800 °C, held at that temperature for 100 h, followed by furnace-cooling to room temperature. The silica tubes were opened in air.

The resulting products were well crystallized with gray color and metallic luster. They are stable in air

| Compound | $CeAgAs_2$ | | $PrAgAs_2$ | $LaAuAs_2$ | | $CeAuAs_2$ | |
|---|---|---|---|---|---|---|---|
| Structure type | $HfCuSi_2$ | | $SrZnSb_2$ | $SrZnBi_2$ | | $HfCuSi_2$ | |
| Formula mass | 397.83 | | 398.62 | 485.72 | | 486.93 | |
| Space group | $P4/nmm$ (No. 129) | | $Pnma$ (No. 62) | $I4/mmm$ (No. 139) | | $P4/nmm$ (No. 129) | |
| Formula units per cell [$Z$] | 2 | | 4 | 4 | | 2 | |
| Pearson symbol | $tP8$ | | $oP16$ | $tI16$ | | $tP8$ | |
| Calculated density [g/cm$^3$] | 7.56 | | 7.67 | 9.01 | | 9.41 | |
| Crystal size [$\mu$m] | $5\times8\times25$ | | $15\times15\times20$ | $10\times10\times50$ | | $10\times10\times30$ | |
| Transmission ratio | 1.67 | | 1.10 | 3.58 | | 3.44 | |
| Highest value $2\theta$ | 70 | | 70 | 80 | | 90 | |
| Range in $hkl$ | $\pm6$, $\pm6$, $-16<l<5$ | | $\pm6$, $\pm6$, $\pm33$ | $\pm7$, $\pm7$, $-36<l<17$ | | $\pm8$, $\pm8$, $\pm20$ | |
| Total no. of reflections | 2157 | | 5674 | 3666 | | 5564 | |
| Unique reflections | 273 | | 849 | 385 | | 473 | |
| Internal residual $R_i(F^2)$ | 0.040 | | 0.133 | 0.077 | | 0.068 | |
| Reflections $F_O>2\sigma$ | 261 | | 746 | 303 | | 428 | |
| Number of variables | 12 | 13 | 26 | 13 | 13 | 12 | 13 |
| Conventional residual ($F_O>2\sigma$) | 0.017 | 0.014 | 0.042 | 0.038 | 0.047 | 0.030 | 0.027 |
| Weighted residual (all $F^2$) | 0.040 | 0.030 | 0.112 | 0.114 | 0.135 | 0.074 | 0.069 |
| Highest/lowest electron density [e/Å$^3$] | 3.1/−2.2 | 3.5/−0.8 | 3.5/−6.8 | 5.9/−4.8 | 8.7/−5.8 | 6.2/−3.5 | 6.4/−2.3 |

Table 2. Crystal data of the arsenides $CeAgAs_2$, $PrAgAs_2$, $LaAuAs_2$, and $CeAuAs_2$. With the exception of $PrAgAs_2$ the structures were also refined with split positions for the As2 atoms. The corresponding results are underlayed with gray color.

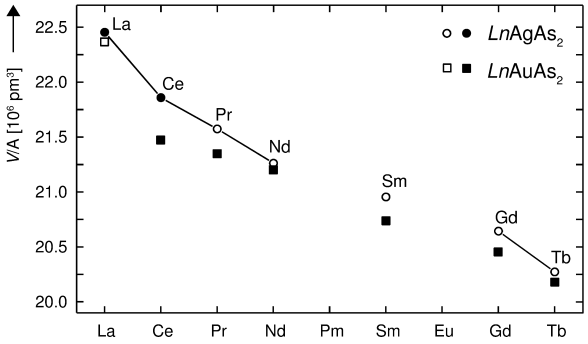


Fig. 1. Average atomic volumes $V$/A of the arsenides $LaAgAs_2$, $CeAgAs_2$, $Ln$AuAs$_2$ ($Ln$ = Ce, Pr, Nd, Sm, Gd, Tb) with $HfCuSi_2$ type structure (filled symbols), $Ln$AgAs$_2$ ($Ln$ = Pr, Nd, Sm, Gd, Tb) with $SrZnSb_2$ type structure, and $LaAuAs_2$ with $SrZnBi_2$ type structure.

for long periods of time. Energy-dispersive X-ray fluorescence analyses in a scanning electron microscope did not show any impurity elements (like silicon) heavier than sodium. Guinier film data of the powdered samples were recorded with Cu-$K_{\alpha1}$ radiation using $\alpha$-quartz ($a$ = 491.30 pm, $c$ = 540.46 pm) as an internal standard. The experimental diagrams were evaluated by comparison with theoretical diagrams calculated [55] on the basis of the structural data resulting from the single-crystal investigations. The lattice constants (Table 1) were obtained by least-squares fits. The average atomic volumes of the ternary arsenides are shown in Fig. 1.

## Structure Determinations

Small crystals of $CeAgAs_2$, $PrAgAs_2$, $LaAuAs_2$, and $CeAuAs_2$ were investigated with an Enraf-Nonius four-circle diffractometer using graphite-monochromated Mo-$K_\alpha$ radiation and a scintillation counter with pulse-height discrimination. The scans were along the Laue streaks ($\omega/2\theta$) with background counts on both ends of each scan. The lattice constants, obtained from the four-circle diffractometer data, were very similar to those from the Guinier powder diagrams (Table 1). They all agreed within less than ten of the (rather small) standard deviations obtained from the powder data. Empirical absorption corrections were applied on the basis of psi-scans. Further details of the data collections and some results are summarized in Table 2.

The structures were solved and refined with the aid of the program systems SHELXTL PLUS [56] and SHELX-97 [57]. The centrosymmetric space groups suggested by the software of the programs were confirmed in all cases during the structure refinements. Most atoms were located by Patterson functions, the remaining ones by difference Fourier syntheses. The structures were refined by a full matrix least-squares program using atomic scattering factors corrected for anomalous dispersion as provided by the program. The weighting schemes reflected the counting statistics and a factor correcting for isotropic secondary extinction was optimized as a least-squares variable. To detect de-

viations from the ideal compositions we refined occupancy values together with variable displacement parameters for all four structures. These varied only between 98(1) and 105(2)%. For that reason we resumed to the ideal occupancy values for the last cycles of the least-squares refinements.

The displacement parameters for the positions of the As2 atoms in the structures of the compounds CeAgAs$_2$, LaAuAs$_2$, and CeAuAs$_2$ were rather large. These structures were subsequently refined with split positions for the As2 atoms. In order to avoid interactions between the displacement and positional parameters these As2 positions had to be refined with isotropic displacement parameters. In the case of the LaAuAs$_2$ structure this raised the residual values *R* as well as the residual electron density. However, the refinement with split As2 position has to be preferred, since the refinement with the As2 atoms in the unsplit position $x = 0$, $y = 1/2$, $z = 0$ had led to an extremely and unrealistically high displacement parameter $U_{11} = 987(40)$ pm$^2$.

The last line of Table 2 lists the highest residual electron densities resulting from difference Fourier syntheses. Most of these values were at locations too close to fully occupied atomic sites and therefore they could be disregarded as possible sites for additional atomic positions. However, there were two exceptions: the residual electron densities of 5.9 e/Å$^3$ in LaAuAs$_2$ and 3.1 e/Å$^3$ in CeAgAs$_2$. Both of these residual electron densities were at locations where additional copper atoms were found in the structures of LaCu$_{1.23(1)}$As$_2$ [40], LaCu$_{1.25(1)}$As$_2$ [41], CeCu$_{1.10(1)}$As$_2$ [40], and CeCu$_{1.11(1)}$As$_2$ [41]. Disregarding the additional copper sites, these arsenides are isotypic with the corresponding compounds LaAuAs$_2$ (SrZnBi$_2$ type) and CeAgAs$_2$ (HfCuSi$_2$ type) reported here. We therefore placed a second Au and Ag atom in these structures and refined their occupancy values, assuming isotropic displacement parameters fixed at the values obtained for the fully occupied Au and Ag positions. The resulting occupancies were very low: 2.3(4) and 1.2(1) %, respectively, corresponding to the formulas LaAu$_{1.023(4)}$As$_2$ and CeAg$_{1.012(1)}$As$_2$. They fit the general tendency of decreasing copper content with decreasing size of the lanthanoid atoms observed in the compounds *Ln*Cu$_{1+x}$As$_2$ [40,41], but might possibly only be the result of insufficient correction of the X-ray data for absorption, which is not reflected in the standard deviations. Thus, LaAuAs$_2$ and CeAgAs$_2$ may be considered to have the ideal compositions within the error limits.

Table 3. Atomic parameters of CeAgAs$_2$ and CeAuAs$_2$ with HfCuSi$_2$ type structure, PrAgAs$_2$ with SrSnSb$_2$ type, and LaAuAs$_2$ with SrZnBi$_2$ type structure. The structures of CeAgAs$_2$, LaAuAs$_2$, and CeAuAs$_2$ were also refined with split positions for the As2 atoms. The resulting atomic parameters for the As2 atoms are underlayed with gray color. The atomic parameters for all other atoms agreed within one standard deviation. Listed are those obtained from the refinements with split As2 positions. The last column contains the equivalent isotropic displacement parameter $U_{eq}$ (pm$^2$) for the metal and As1 atoms. For the As2 atoms the first (high) value corresponds to the equivalent displacement parameter obtained during the refinement with unsplit As2 positions; the second (lower) value listed in the next line is the isotropic *U* value resulting from the refinement with split As2 position.

| CeAgAs$_2$ | *P*4/*nmm* | *x* | *y* | *z* | $U_{eq}$ or *U* |
|---|---|---|---|---|---|
| Ce | 2*c* | 1/4 | 1/4 | 0.23104(3) | 86(1) |
| Ag | 2*b* | 3/4 | 1/4 | 1/2 | 117(1) |
| As1 | 2*c* | 1/4 | 1/4 | 0.67684(6) | 87(2) |
| As$_2$ | 2*a* | 3/4 | 1/4 | 0 | 277(3) |
| As$_2$ | 8*i* | 0.6958(3) | 1/4 | 0.0017(3) | 81(2) |
| PrAgAs$_2$ | *Pnma* | | | | |
| Pr | 4*c* | 0.11571(3) | 1/4 | 0.7253(1) | 46(2) |
| Ag | 4*c* | 0.25021(4) | 1/4 | 0.2244(2) | 86(2) |
| As1 | 4*c* | 0.0161(6) | 1/4 | 0.2016(3) | 77(2) |
| As$_2$ | 4*c* | 0.33884(6) | 1/4 | 0.7247(2) | 55(2) |
| LaAuAs$_2$ | *I*4/*mmm* | | | | |
| La | 4*e* | 0 | 0 | 0.11850(8) | 92(3) |
| Au | 4*d* | 0 | 1/2 | 1/4 | 138(3) |
| As1 | 4*e* | 0 | 0 | 0.3362(1) | 87(5) |
| As$_2$ | 4*c* | 0 | 1/2 | 0 | 462(13) |
| As$_2$ | 16*l* | 0.051(1) | 0.469(2) | 0 | 155(13) |
| CeAuAs$_2$ | *P*4/*nmm* | | | | |
| Ce | 2*c* | 1/4 | 1/4 | 0.23430(6) | 81(1) |
| Au | 2*b* | 3/4 | 1/4 | 1/2 | 132(1) |
| As1 | 2*c* | 1/4 | 1/4 | 0.6800(1) | 84(2) |
| As$_2$ | 2*a* | 3/4 | 1/4 | 0 | 288(4) |
| As$_2$ | 8*i* | 0.6957(4) | 1/4 | 0.0013(3) | 68(4) |

The positional parameters of the refinements with unsplit atomic positions were standardized using the program STRUCTURE TIDY [58]. The results of all refinements are summarized in the Tables 2 and 3. They have also been deposited and may be obtained from the Fachinformationszentrum Karlsruhe GmbH, D-76344 Eggenstein-Leopoldshafen by quoting the registry numbers CSD-412819 (CeAgAs$_2$), CSD-412816 (PrAgAs$_2$), CSD-412818 (LaAuAs$_2$), and CSD-412817 (CeAuAs$_2$).

## Discussion

The various arsenides reported here are represented by their average atomic volumes in Fig. 1. Gener-

Table 4. Interatomic distances in the structure of PrAgAs$_2$. All distances shorter than 380 pm are listed. Standard deviations are all less or equal 0.2 pm.

| | | | | | | | | |
|---|---|---|---|---|---|---|---|---|
| Pr: | 2Ag | 346.7 | Ag: | 2Pr | 346.7 | As1: | Pr | 309.1 |
| | Ag | 348.9 | | Pr | 348.9 | | 2Pr | 319.9 |
| | Ag | 349.4 | | Pr | 349.4 | | Pr | 321.6 |
| | 2As2 | 301.6 | | 4Ag | 286.2 | | 2As1 | 259.6 |
| | 2As2 | 302.0 | | 2As2 | 274.9 | | 2As1 | 315.7 |
| | As1 | 309.1 | | As2 | 276.4 | As2: | 2Pr | 301.6 |
| | 2As1 | 319.9 | | As2 | 276.6 | | 2Pr | 302.0 |
| | As1 | 321.6 | | | | | 2Ag | 274.9 |
| | | | | | | | Ag | 276.4 |
| | | | | | | | Ag | 276.6 |

ally, these volumes follow smooth functions, reflecting the well-known lanthanoid contraction, irregardless of their differing (albeit closely related) crystal structures. The silver-containing arsenides have slightly larger average atomic volumes than the corresponding gold compounds. The average atomic volume of the gold compound CeAuAs$_2$, however, is considerably smaller than that of the corresponding silver compound CeAgAs$_2$. This suggests mixed or intermediate III/IV valence of the cerium atoms in the gold compound, thus reflecting the higher electronegativity of gold as compared to that of silver.

The compounds reported here crystallize with three different, very closely related structures first determined for HfCuSi$_2$ [1], SrZnSb$_2$ [32], and SrZnBi$_2$ [33]. The HfCuSi$_2$ type structure has variously also been designated as ZrCuSi$_2$ type [59], CaMnBi$_2$ type [60], and UCuAs$_2$ type [61]. All of these structures may be regarded as belonging to a large family of tetragonal structures of which those of PbClF and ThCr$_2$Si$_2$ are probably the best known members. The reader is referred to earlier publications for various aspects of crystal chemical and topological relationships between these structures [2, 27, 34, 41, 60, 62 – 70].

For the five arsenides *Ln*AgAs$_2$ (*Ln* = Pr, Nd, Sm, Gd, Tb) we found the orthorhombic SrZnSb$_2$ type structure [32], which we refined for PrAgAs$_2$. We will discuss this structure first, since the structure refinement resulted in well localized positions for all atoms, as can be judged from the relatively low and similar displacement parameters of all atoms (Table 3). This structure and the near-neighbor coordinations are shown in Fig. 2. The praseodymium atoms are located in a distorted square-antiprism formed by both As1 and As2 atoms. Four silver atoms outside the square face formed by the As2 atoms are at distances of between 346.7 and 349.4 pm (Table 4). These near-neighbor

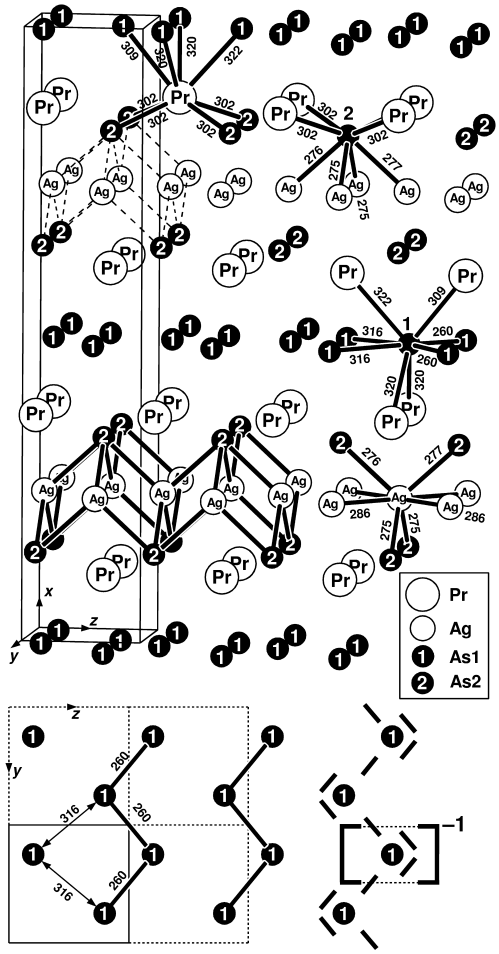


Fig. 2. Crystal structure and near-neighbor coordinations in the arsenide PrAgAs$_2$ with orthorhombic SrZnSb$_2$ type structure. Some interatomic distances (pm) are indicated with three-digit numbers. While the As2 atoms are isolated from each other, the As1 atoms form a very distorted square grid with two short and two long As1–As1 distances for each As1 atom. In a first approximation the As1 atoms may be considered to form zigzag chains where they obtain the formal charge −1, as can be seen from the Lewis formula in the lower right-hand corner.

interactions may be considered as only very weakly bonding (at best) in view of the fact that the sum of the "metallic" radii (for the coordination number CN 12) amounts to 327.3 pm [71].

The silver atoms have distorted tetrahedral arsenic coordination with four additional silver neighbors at 286.2 pm. This distance is close to the Ag–Ag distance of 288.9 pm calculated from the lattice constant of the cubic close packed structure (CN 12) of elemental silver [72].

Of the two different arsenic atoms, the As2 atoms have only metal neighbors forming a distorted square antiprism (Fig. 2). Using oxidation numbers, where the electrons of the more or less covalent Ag–As and Pr–As bonds are counted at the partner with the greater electronegativity, these arsenic atoms can be assigned the formal charge $-3$ (octet rule; because of the high electronegativity of the arsenic atoms their 4s and 4p orbitals will fully participate in bonding with the metal atoms). In contrast, the As1 atoms have four As1 neighbors: two at 259.6 pm and two at 315.7 pm. These distances may be compared with the As–As distances in elemental $\alpha$-arsenic [72] of 251.7 pm ($3\times$) and 312.0 pm ($3\times$). In a very simple bonding description of elemental arsenic the short As–As bonds of 251.7 pm may be considered as single (two-electron) bonds (bond order one), while the longer bonds of 312.0 pm may be regarded as weak "van der Waals" interactions (bond order zero). Both of these distances are slightly shorter than the two As1–As1 distances of 259.6 and 315.7 pm in PrAgAs$_2$. However, for simplicity and in aiming for integral numbers we can assign a bond order of one to the As1–As1 bonds of 259.6 pm. In this way the As1 atoms obtain the oxidation number $-1$, as shown with the Lewis formula in the lower right-hand part of Fig. 2. If we allow fractional bonds, as recently discussed for rare earth polyantimonides [73], we can assign a bond order of (say) 0.75 to the As1–As1 bonds of 259.6 pm and a bond order of 0.25 to the As1–As1 bonds of 315.7 pm. This would not change the formal charge of $-1$ for the As1 atoms. Hence, chemical bonding in this compound may very roughly be represented by the formula $Pr^{+3}Ag^{+1}As1^{-1}As2^{-3}$. We note that this formula does not account for the weak Ag–Ag bonding mentioned above. If we want to account for that, we have to assume a higher valency for the silver atoms (as is well known for copper and gold) or we have to retain some electrons on the silver atoms to fill a Ag–Ag bonding band, thus reducing the formal charge of the silver atoms and also the absolute value of the charge on the As1 atoms.

Most of the arsenides reported here crystallize with HfCuSi$_2$ type structure. We have refined this structure for the two cerium compounds CeAgAs$_2$ and CeAuAs$_2$, and show it in Fig. 3 with CeAgAs$_2$ as example. In comparing the interatomic distances of the two isotypic compounds CeAgAs$_2$ and CeAuAs$_2$ (Table 5) we note that almost all corresponding distances agree within 0.8% or less. The only exception

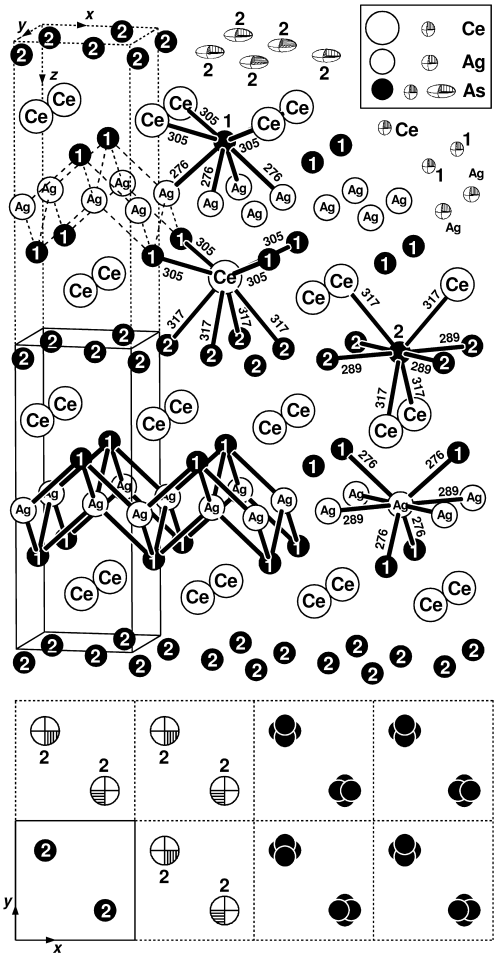


Fig. 3. The tetragonal HfCuSi$_2$ type structure of CeAgAs$_2$. To facilitate comparisons with the structure of PrAgAs$_2$ (Fig. 2) two unit cells are shown on top of each other. Single-digit numbers correspond to the designations of the As1 and As2 atoms; three-digit numbers indicate interatomic distances in pm units. In the upper right-hand corner some atoms are represented by their displacement ellipsoids at the 90% probability limit. In the lower right-hand corner the positions of the As2 atoms are shown as resulting from the refinement with split atomic positions.

is the marginally bonding Ce–Ag distance of 348.1 pm which corresponds to the Ce–Au distance of 339.2 pm. This difference might possibly result from a larger fraction of Ce(IV) atoms in the gold compound due to the higher electronegativity of gold as compared to that of silver as already discussed above.

The near-neighbor environments of the HfCuSi$_2$ type arsenides CeAgAs$_2$ and CeAuAs$_2$ on the one hand, and those of PrAgAs$_2$ with SrZnSb$_2$ type structure on the other, are very similar, as can be seen by a

Table 5. Interatomic distances in the isotypic arsenides CeAgAs$_2$ and CeAuAs$_2$. All distances shorter than 360 pm are listed. Standard deviations are all less or equal to 0.3 pm. The structure was refined with unsplit and with split positions for the As2 atoms. Interatomic distances for the two refinements differ by less than one standard deviation except for distances involving As2 atoms. The upper part of the table contains the distances corresponding to the refinements with nonsplit As2 positions; the lower part lists only those distances which result through the splitting of the As2 positions, now having occupancy values of only 25%. Corresponding distances in the two compounds are given in the sequence CeAgAs$_2$/CeAuAs$_2$.

| | | | | | |
|---|---|---|---|---|---|
| Nonsplit As2 positions | | | | | |
| Ce: | 4Ag/Au | 348.1/339.2 | As1: | 4Ce | 304.6/303.6 |
| | 4As1 | 304.5/303.6 | | 4Ag/Au | 275.8/275.1 |
| | 4As2 | 316.8/314.5 | | | |
| Ag/Au: | 4Ce | 348.1/339.2 | As2: | 4Ce | 316.8/314.5 |
| | 4Ag/Au | 288.8/290.9 | | 4As2 | 288.8/290.9 |
| | 4As1 | 275.8/275.1 | | | |
| Split As2 positions | | | | | |
| Ce: | 4As2 | 301.6/299.3 | As2: | 1Ce | 301.6/299.3 |
| | 8As2 | 318.9/316.3 | | 2Ce | 318.9/316.3 |
| | 4As2 | 330.2/328.5 | | 1Ce | 330.2/328.5 |
| | | | | 2As2 | 257.5/259.3 |
| | | | | 2As2 | 259.4/261.3 |
| | | | | 4As2 | 288.8/290.9 |
| | | | | 4As2 | 290.5/292.6 |
| | | | | 2As2 | 320.2/322.4 |
| | | | | 2As2 | 321.7/324.0 |

comparison of Figs. 2 and 3. For this comparison we have to keep in mind that the atom designations of the As1 and As2 atoms have to be interchanged (the near-neighbor coordinations of the As2 atoms in PrAgAs$_2$ correspond to those of the As1 atoms in CeAgAs$_2$). The differences between the structures result from the shifts of atomic layers perpendicular to the long translation period (the *x* axis in PrAgAs$_2$ and the *z* axis of CeAgAs$_2$). The main difference in the near-neighbor coordinations of the two structures is due to the fact that both structure refinements for the two isotypic cerium compounds could be carried out with split positions for the As2 atoms, while the corresponding As1 atoms of PrAgAs$_2$ were found to be well localized.

In the structure of CeAgAs$_2$ refined with nonsplit As2 positions the As2 atoms have large displacement parameters in the *xy* plane. They form a square net, where each As2 atom has four As2 neighbors at the weakly bonding distance of 288.8 pm. This might well be a good description for a high-temperature form of the compound. However, the structure refinement from X-ray data recorded at room temperature is better carried out with split As2 positions. This shows that the As2 atoms have moved off their mean positions similar to the situation called a Jahn-Teller distortion in molecular chemistry or a Peierls distortion in extended solids [69]. The As2 atoms may now form two relatively strong and two very weak As2–As2 bonds similar to the environments discussed above for the As1 atoms in PrAgAs$_2$ (Table 4, Fig. 2). In Fig. 4 we show a cut through the structure of CeAgAs$_2$ at the height of the split positions of the As2 atoms. Two simple models of high symmetry for the order of occupied and nonoccupied As2 sites are shown: one where the As2 atoms form squares and one where they form zigzag chains. If chains are formed, the unit cell does not need to be enlarged; only the rotational (as opposed to translational) symmetry is lowered from tetragonal to orthorhombic. If the As2 atoms form squares, the tetragonal symmetry can be retained with a $\sqrt{2}$ times larger *a* axis.

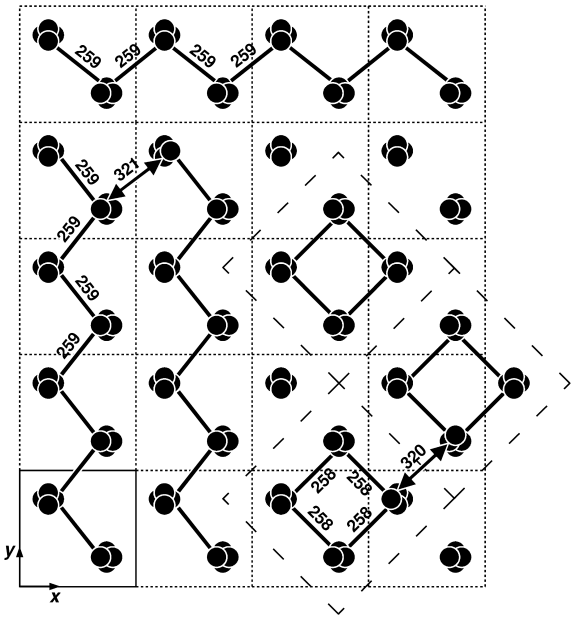


Fig. 4. Models for the order of occupied and nonoccupied As2 positions in the structure of CeAgAs$_2$. The tetragonal cell of the HfCuSi$_2$ type structure is outlined in the lower left-hand corner. Occupied As2 positions might form chains or rings with As2–As2 distances of 259.4(1) pm or 257.5(2) pm, respectively. In the latter case the a axis of the tetragonal cell would be enlarged by a factor of $\sqrt{2}$ (dashed lines). The formation of chains lowers the symmetry to orthorhombic, where the two translation periods *a* and *b* (dotted lines) do not need to be equal. More complicated patterns with larger translation periods are possible, but less likely.

In both cases – chains or squares of As2 atoms – each As2 atom has two relatively strongly bonded As2

Table 6. Interatomic distances in the structure of LaAuAs$_2$. This structure has been refined with full occupancy for all atomic positions and also with split As2 positions each with an occupancy of 25%. Most interatomic distances of the two refinements differ by less than one standard deviation. Exceptions are the distances to and between As2 atoms. In the lower part of the table only those distances are listed which result from the splitting of the As2 positions. All distances shorter than 370 pm are listed. Standard deviations are all less than 0.2 pm for the distances with unsplit positions, less than 0.6 pm for the La atoms to the split As2 positions, and less than 1.3 pm for distances between split As2 positions.

| | | | | | |
|---|---|---|---|---|---|
| Nonsplit As2 positions | | | | | |
| La: | 4Au | 342.0 | As1: | 4La | 309.2 |
| | 4As1 | 309.2 | | 4Au | 273.9 |
| | 4As2 | 320.8 | | | |
| Au: | 4La | 342.0 | As2: | 4La | 320.8 |
| | 4Au | 294.8 | | 4As2 | 294.8 |
| | 4As1 | 273.9 | | | |
| Split As2 positions | | | | | |
| La: | 8As2 | 313.5 | | | |
| | 8As2 | 330.2 | | | |
| As2: | 2La | 313.5 | As2: | 2As2 | 295.0 |
| | 2La | 330.2 | | 2As2 | 298.7 |
| | 1As2 | 246.4 | | 1As2 | 306.6 |
| | 2As2 | 265.3 | | 2As2 | 314.5 |
| | 2As2 | 278.2 | | 2As2 | 325.4 |
| | 1As2 | 283.0 | | 1As2 | 343.2 |

neighbors at distances of 259.4(1) or 257.5(2) pm, respectively. The other two As2 neighbors are then at 321.7(2) or 320.2(2) pm, respectively. Thus, the As2–As2 bonding situation in CeAgAs$_2$ is similar to that of the As1–As1 bonding discussed above for PrAgAs$_2$. In a first approximation, we can assign to each As2 atom for the two relatively close As2 neighbors and the two other very weakly bonded As2 neighbors a total bond order of 2, corresponding to the oxidation number $-1$. We thus obtain a formula with the formal charges balanced according to $Ce^{+3}Ag^{+1}As1^{-3}As2^{-1}$ similar to that of $Pr^{+3}Ag^{+1}As1^{-1}As2^{-3}$.

The fourth structure we have refined is that of LaAuAs$_2$ which is isotypic with the body centered tetragonal structure of the bismuthide SrZnBi$_2$. As compared to the tetragonal HfCuSi$_2$ type structure (Fig. 3), found for the other ternary gold arsenides *Ln*AuAs$_2$, the structure of LaAuAs$_2$ has a doubled *c* axis. This doubling is associated with a minor plane perpendicular to the tetragonal axis located at the height of the As2 atoms. As a consequence, the As2 atoms are situated in a rectangle of La atoms in contrast to the As2 atoms in the HfCuSi$_2$ type arsenides where the As2 atoms have (slightly elongated) tetrahedral *Ln* coordination. The environments of the other

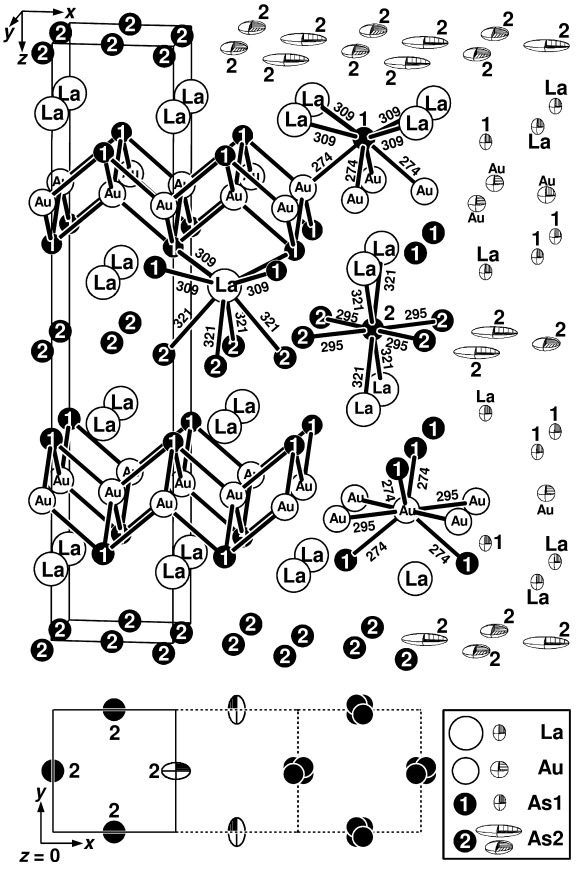


Fig. 5. The body centered tetragonal SrZnBi$_2$ type structure of LaAuAs$_2$. Some displacement ellipsoids are shown with their 90% probability limits. Interatomic distances are given in pm units. At the bottom a layer of As2 atoms at $z = 0$ is drawn indicating their split positions and their corresponding displacement ellipsoids resulting from a least-squares refinement with unsplit positions.

three atomic positions correspond to those already discussed for PrAgAs$_2$ (Fig. 2) and CeAgAs$_2$ (Fig. 3).

The refinement of the As2 positions of LaAuAs$_2$ showed again very high anisotropic displacement parameters with their largest displacements perpendicular to the *z* axis of the tetragonal cell. However, in contrast to the refinements for the As2 positions of CeAgAs$_2$ and CeAuAs$_2$, it was not possible to obtain a perfectly satisfactory result assuming only one split position. The best result, shown in Table 3 (As2 of 4*c* with $U_{eq}$ = 462 pm$^2$ splits to 16*l* with $U_{iso}$ = 155 pm$^2$), has still a relatively large isotropic displacement parameter for the 16*l* position of As2. It seems possible that the crystal has domains, where a splitting of the 4*c* position to the position 8*i*, or the equivalent 8*j*, might

be a more fitting description. The refinements of the whole structure with these positions gave less satisfactory results. In principle, with the proper constraints, it is possible to refine the structure also with two different split positions for the As2 atoms. However, we have not attempted to resort to such complicated solutions. It is clear that the locations of the As2 atoms are off the highly symmetric 4*c* position with the local symmetry *mmm*. Thus, the As2 atoms in LaAuAs$_2$ very likely form rings or chains similar to those indicated for the As2 atoms of CeAgAs$_2$ shown in Fig. 4. Consequently, they can again be assigned the formal charge of $-1$, and chemical bonding of the gold compound can be rationalized to a first approximation with the analogous formula $La^{+3}Au^{+1}As1^{-3}As2^{-1}$.

The gold containing compounds *Ln*AuAs$_2$ reported here crystallize with the same structures (SrZnBi$_2$ type for the lanthanum compounds, HfCuSi$_2$ type for the others) as those refined from single-crystal data for the corresponding ternary copper arsenides *Ln*Cu$_{1+x}$As$_2$ [40,41], if we disregard the small excess copper contents found for some of the latter. If these additional copper positions were completely filled, these structures would correspond to that of CaBe$_2$Ge$_2$ [62]. However, since the excess copper contents are low, these structures might better be described as "filled" SrZnBi$_2$ type and HfCuSi$_2$ type, respectively [40, 41]. It is interesting that the excess copper content $x$ of *Ln*Cu$_{1+x}$As$_2$ is decreasing systematically with the size of the rare earth atoms in the sequence $x = 0.23(1)$ [40] and $x = 0.25(1)$ [41] for *Ln* = La, $x = 0.10(1)$ [40] and 0.11(1) [41] for *Ln* = Ce, $x = 0.09(1)$ for *Ln* = Pr [40], $x = 0.06(1)$ for *Ln* = Nd [41], $x = 0.05(1)$ for *Ln* = Sm [41], to $x$ = zero for *Ln* = Ho [40] and *Ln* = Yb [41]. In two of our present structure refinements (for LaAuAs$_2$ and CeAgAs$_2$) could we observe small residual electron densities (corresponding to $x = 0.023(4)$ and $x = 0.012(1)$, respectively), however, as discussed above, these are within the error limits.

We would like to point out that the decreasing copper content reported for these compounds can be rationalized on the basis of the simple bonding model discussed above for the silver and gold containing compounds. With decreasing size of the rare earth atoms, the lattice constants $a$ of the tetragonal cells decrease; this decrease results in shorter As2–As2 bonds. Increasing As–As bonding means lowering the absolute value of the formal charge of the As atoms (arsenic atoms with an equivalent of three two-electron As–As bonds have a formal charge of zero; if the arsenic atoms are isolated from each other they have a formal charge of $-3$). Thus, the longer the As2–As2 bonds, the more positive formal charges from the additional copper atoms can be compensated by the As2 polyanions. One could argue that the $a$ axis in the silver and gold compounds *Ln*AgAs$_2$ and *Ln*AuAs$_2$ is larger than in the copper compounds, and therefore the silver and gold compounds should accommodate also and even more additional silver and gold in "filled" compounds *Ln*Ag$_{1+x}$As$_2$ and *Ln*Au$_{1+x}$As$_2$. In contrast to this expectation, these compounds were found by us to have the ideal 1:1:2 composition. However, this apparent discrepancy can be rationalized by the fact that silver and gold in these compounds might be strictly monovalent, whereas copper in these arsenides might be partially divalent. The tendency for the divalent state is well known for copper.

*Acknowledgements*

We thank Dr. M. H. Möller for important preliminary work on the silver containing arsenides reported here. We acknowledge Dipl.-Ing. U. Ch. Rodewald for the competent collection of the single-crystal diffractometer data and Mr. H.-J. Göcke for the engaged work at the scanning electron microscope. We are indebted to Dr. W. Gerhartz (Degussa) and Dr. G. Höfer (Heraeus Quarzschmelze, Hanau) for generous gifts of gold wire and silica tubes, respectively. This work was also supported by the Deutsche Forschungsgemeinschaft, the Fonds der Chemischen Industrie, and the International Centre for Diffraction Data.

[1] L. S. Andrukhiv, L. A. Lysenko, Ya. P. Yarmolyuk, E. I. Gladyshevskii, Dopov. Akad. Nauk Ukr. RSR, Ser. A, p. 645 (1975).
[2] V. Johnson, W. Jeitschko, J. Solid State Chem. **11**, 161 (1974).
[3] P. Villars, L. D. Calvert, Pearson's Handbook of Crystallographic Data for Intermetallic Phases. Materials Information Society, Materials Park, Ohio (1991).
[4] E. Parthé, L. Gelato, B. Chabot, M. Penzo, K. Cenzual, R. Gladyshevskii, TYPIX, Standardized Data and Crystal Chemical Characterization of Inorganic Structure Types, Volumes 1 – 4, Gmelins Handbook of Inorganic and Organometallic Chemistry. Springer, Berlin (1993).
[5] K. R. Andress, E. Alberti, Z. Metallkd. **27**, 126 (1935).
[6] Z. Ban, M. Sikirica, Acta Crystallogr. **18**, 594 (1965).

[7] P. M. Raccah, J. M. Longo, H. A. Eick, Inorg. Chem. **6**, 1471 (1967).
[8] R. Benz, W. H. Zachariasen, Acta Crystallogr. **B26**, 823 (1970).
[9] W. Jeitschko, B. Jaberg, J. Solid State Chem. **35**, 312 (1980).
[10] W. B. Pearson, J. Solid State Chem. **56**, 278 (1985).
[11] G. Just, P. Paufler, J. Alloys Compd. **232**, 1 (1996).
[12] P. Villars, Pearson's Handbook Desk Edition. Materials Information Society, Materials Park, Ohio (1997).
[13] F. A. Weber, Th. Schleid, Z. Anorg. Allg. Chem. **625**, 1833 (1999).
[14] M. Brylak, M. H. Möller, W. Jeitschko, J. Solid State Chem. **115**, 305 (1995).
[15] P. Quebe, L. J. Terbüchte, W. Jeitschko, J. Alloys Compd. **302**, 70 (2000).
[16] B. A. Popovkin, A. M. Kusainova, V. A. Dolgikh, L. G. Aksel'rud, Russ. J. Inorg. Chem. **43**, 1471 (1998).
[17] P. Lauxmann, Th. Schleid, Z. Anorg. Allg. Chem. **626**, 2253 (2000).
[18] A. T. Nientiedt, W. Jeitschko, Inorg. Chem. **37**, 386 (1998).
[19] D. O. Charkin, P. S. Berdonosov, V. A. Dolgikh, P. Lightfoot, J. Alloys Compd. **292**, 118 (1999).
[20] H. Grossholz, Th. Schleid, Z. Kristallogr. Suppl. **19**, 104 (2002).
[21] H. Grossholz, Th. Schleid, Z. Anorg. Allg. Chem. **628**, 2169 (2002).
[22] H. Abe, K. Yoshii, J. Solid State Chem. **165**, 372 (2002).
[23] A. Mewis, Z. Naturforsch. **35b**, 141 (1980).
[24] M. H. Möller, Darstellung, Kristallstrukturen und Eigenschaften binärer und ternärer Pnictide der Münzmetalle, Dissertation, Universität Dortmund (1983).
[25] M. H. Möller, W. Jeitschko, Acta Crystallogr. **A37** (Suppl.), 176 (1981).
[26] M. H. Möller, W. Jeitschko, Ternary Rare Earth Copper and Silver Pnictides with $ThCr_2Si_2$-related Structures, in VIIIth Int. Conf. on Solid Compounds of Transition Elements, Extended Abstracts, P4, A15 Vienna, Austria (1985).
[27] Yu. B. Kuz'ma, St. Chykhrij, in K. A. Gschneidner (Jr.), L.-R. Eyring (eds): Handbook on the Physics and Chemistry of Rare Earths, Vol. **23**, pp. 285 – 434, North Holland (Elsevier), Amsterdam (1996).
[28] Yu. B. Kuz'ma, R. Demchyna, H. Borrmann, A. Rabis, W. Schnelle, S. Chykhrij, Yu. Grin, Z. Anorg. Allg. Chem. **628**, 2178 (2002).
[29] St. I. Chykhrij, Zh. Neorg. Khim. **35**, 1656 (1990).
[30] St. I. Chykhrij, G. V. Loukashouk, S. V. Oryshchyn, Yu. B. Kuz'ma, J. Alloys Compd. **248**, 224 (1997).
[31] R. O. Demchyna, S. V. Oryshchyn, Yu. B. Kuz'ma, J. Alloys Compd. **322**, 176 (2001).
[32] E. Brechtel, G. Cordier, H. Schäfer, Z. Naturforsch. **34b**, 251 (1979).
[33] G. Cordier, B. Eisenmann, H. Schäfer, Z. Anorg. Allg. Chem. **426**, 205 (1976).
[34] Th. Ebel, W. Jeitschko, J. Solid State Chem. **116**, 307 (1995).
[35] A. T. Nientiedt, W. Jeitschko, J. Solid State Chem. **142**, 266 (1999).
[36] R. Demchyna, H. Borrmann, St. I. Chykhrij, Yu. B. Kuz'ma, Yu. Grin, Z. Kristallogr. NCS **217**, 161 (2002).
[37] Yu. Mozharivskyj, A. O. Pecharsky, S. Bud'ko, H. F. Franzen, Z. Anorg. Allg. Chem. **628**, 1619 (2002).
[38] Yu. Mozharivskyj, D. Kaczorowski, H. F. Franzen, J. Solid State Chem. **155**, 259 (2000).
[39] Yu. Mozharivskyj, D. Kaczorowski, H. F. Franzen, Z. Anorg. Allg. Chem. **627**, 2163 (2001).
[40] M. Wang, R. McDonald, A. Mar, J. Solid State Chem. **147**, 140 (1999).
[41] J.-P. Jemetio, Th. Doert, O. Rademacher, P. Böttcher, J. Alloys Compd. **338**, 93 (2002).
[42] J. P. F. Jemetio, Th. Doert, O. Rademacher, P. Böttcher, Z. Anorg. Allg. Chem. **628**, 2175 (2002).
[43] O. Sologup, K. Hiebl, P. Rogl, H. Noël, O. I. Bodak, J. Alloys Compd. **210**, 153 (1994).
[44] Y. Muro, N. Takeda, M. Ishikawa, J. Alloys Compd. **257**, 23 (1997).
[45] M. Kolenda, M. Hofmann, J. Leciejewicz, B. Penc, A. Szytuła, A. Zygmunt, J. Alloys Compd. **315**, 22 (2001).
[46] M. Kolenda, A. Oleś, A. Szytuła, J. Alloys Compd. **322**, 55 (2001).
[47] G. Cordier, H. Schäfer, P. Woll, Z. Naturforsch. **40b**, 1097 (1985).
[48] J. Ye, Y. K. Huang, K. Kadowaki, T. Matsumoto, Acta Crystallogr. **C52**, 1323 (1996).
[49] O. Sologup, H. Noël, A. Leithe-Jasper, P. Rogl, O. I. Bodak, J. Solid State Chem. **115**, 441 (1995).
[50] K. D. Myers, S. L. Bud'ko, V. P. Antropov, B. N. Harmon, P. C. Canfield, A. H. Lacerda, Phys. Rev. B **60**, 13371 (1999).
[51] K. D. Myers, S. L. Bud'ko, I. R. Fisher, Z. Islam, H. Kleinke, A. H. Lacerda, P. C. Canfield, J. Magn. Magn. Mater. **205**, 27 (1999).
[52] L. Zeng, X. Xie, H. F. Franzen, J. Alloys Compd. **343**, 122 (2002).
[53] P. Wollesen, W. Jeitschko, M. Brylak, L. Dietrich, J. Alloys Compd. **245**, L5 (1996).
[54] R. O. Demchyna, Yu. B. Kuz'ma, V. S. Babizhetsky, J. Alloys Compd. **315**, 158 (2001).

[55] K. Yvon, W. Jeitschko, E. Parthé, J. Appl. Crystallogr. **10**, 73 (1977).
[56] G. M. Sheldrick, SHELXTL PLUS, Release 4.21/V, Siemens Analytical Instruments Inc., Madison, Wisconsin, USA (1990).
[57] G. M. Sheldrick, SHELX-97. A Program System for Solving and Refining Crystal Structures. Universität Göttingen, Germany (1997).
[58] L. M. Gelato, E. Parthé, J. Appl. Crystallogr. **20**, 139 (1987).
[59] F. Thirion, G. Venturini, B. Malaman, J. Steinmetz, B. Roques, J. Less-Common Met. **95**, 47 (1983).
[60] E. Brechtel, G. Cordier, H. Schäfer, Z. Naturforsch. **35b**, 1 (1980).
[61] J. Stępień-Damm, D. Kaczorowski, R. Troć, J. Less-Common Met. **132**, 15 (1987).
[62] B. Eisenmann, N. May, W. Müller, H. Schäfer, Z. Naturforsch. **27b**, 1155 (1972).
[63] E. Parthé, B. Chabot, H. F. Braun, N. Engel, Acta Crystallogr. **B39**, 588 (1983).
[64] Ch. Zheng, R. Hoffmann, J. Am. Chem. Soc. **108**, 3078 (1986).
[65] W. Tremel, R. Hoffmann, J. Am. Chem. Soc. **109**, 124 (1987).
[66] E. H. El Ghadraoui, J. Y. Pivan, R. Guérin, J. Less-Common Met. **136**, 303 (1988).
[67] J. H. Albering, W. Jeitschko, Z. Naturforsch. **51b**, 257 (1996).
[68] D. Kußmann, R. Pöttgen, U. Ch. Rodewald, C. Rosenhahn, B. D. Mosel, G. Kotzyba, B. Künnen, Z. Naturforsch. **54b**, 1155 (1999).
[69] G. A. Papoian, R. Hoffmann, Angew. Chem. **112**, 2500 (2000).
[70] M. W. Pohlkamp, W. Jeitschko, Z. Naturforsch. **56b**, 1143 (2001).
[71] E. Teatum, K. Gschneidner, J. Waber, LA-2345, U.S. Department of Commerce, Washington, D. C. (1960). See W. B. Pearson, The Crystal Chemistry and Physics of Metals and Alloys, Wiley, New York (1972).
[72] J. Donohue, The Structures of the Elements, Wiley New York (1974).
[73] W. Jeitschko, R. O. Altmeyer, M. Schelk, U. Ch. Rodewald, Z. Anorg. Allg. Chem. **627**, 1932 (2001).